GLIA 58:114–124 (2010)

Involvement of Cathepsin B in the Processing and Secretion of Interleukin-1β in Chromogranin A-Stimulated Microglia

KAYO TERADA,[1] JUN YAMADA,[1] YOSHINORI HAYASHI,[1] ZHOU WU,[1] YASUO UCHIYAMA,[2] CHRISTOPH PETERS,[3] AND HIROSHI NAKANISHI[1]*

[1]*Department of Aging Science and Pharmacology, Faculty of Dental Sciences, Kyushu University, Fukuoka 812-8582, Japan*
[2]*Department of Cell Biology and Neuroscience, Juntendo University Graduate School of Medicine, Tokyo, Japan*
[3]*Institut für Molekulare Medizin und Zellforshung, Albert-Ludwings-Universität Freiburg Hugstetter Strasse 55, 79106 Freiburg, Germany*

KEY WORDS
microglia; cathepsin B; interleukin-1β; chromogranin A; caspase-1; processing; lysosomes

ABSTRACT
Cathepsin B (CB) is a cysteine lysosomal protease implicated in a number of inflammatory diseases. Although it is now evident that caspase-1, an essential enzyme for maturation of interleukin-1β (IL-1β), can be activated through the inflammasome, there is still evidence suggesting the existence of lysosomal-proinflammatory caspase pathways. In the present study, a marked induction of pro-IL-1β, its processing to the mature form and secretion were observed in the primary cultured microglia prepared from wild-type mice after stimulation with chromogranin A (CGA). Although pro-IL-1β also markedly increased in microglia prepared from CB-deficient mice, CB-deficiency abrogated the pro-IL-1β processing. CA-074Me, a specific inhibitor for CB, inhibited the pro-IL-1β maturation and its release from microglia. Furthermore, the caspase-1 activation was also inhibited by CA-074Me and E-64d, a broad cysteine protease inhibitor. After treatment with CGA, CB was markedly induced at both protein and mRNA levels. The induced pro-CB was rapidly processed to its mature form. The immunoreactivity for CB co-localized with both that for caspase-1 and the cleaved IL-1β, in the acidic enlarged lysosomes. In consistent with these *in vitro* observations, the immunoreactivity for the cleaved IL-1β was markedly observed in microglia of the hippocampus from aged wild-type but not CB-deficient mice. These observations strongly suggest that CB plays a key role in the pro-IL-1β maturation through the caspase-1 activation in enlarged lysosomes of CGA-treated microglia. Therefore, either pharmacological or genetic inhibition of CB may provide therapeutic intervention in inflammation-associated neurological diseases.

INTRODUCTION

There is substantial evidence that cathepsin B (CB, EC 3.4.22.1), a typical cysteine lysosomal protease, is markedly upregulated in activated microglia that accumulate in pathological sites of the brain. However, little information is available about the precise function of CB expressed in these activated microglia. Besides lysosomal bulk proteolysis, CB has specific roles in microglia including proteolytic processing of the invariant chain of MHC II in microglia (Nakanishi, 2003; Nishioku et al., 2002). Beyond its functions in the endosomal/lysosomal system, CB can be secreted from activated microglia as the mature form to induce neuronal apoptosis (Gan et al., 2004; Kingham and Pocock, 2001) and degrade β-amyloid peptides that accumulate in the brain (Mueller-Steiner et al., 2006).

It is also thought that CB plays an essential role in inflammatory response in the brain initiated by activated microglia, because CB is implicated in a number of peripheral inflammatory diseases including bronchial disease (Cardozo et al., 1992) and rheumatoid arthritis (Hashimoto et al., 2001). Interleukin-1β (IL-1β) is a potent proinflammatory cytokine that plays a key role in the pathogenesis of diverse range of neurological diseases including Alzheimer's disease, Parkinson's disease, stroke (Allan et al., 2005), and persistent pain (Guo et al., 2007; Kawasaki et al., 2008; Samad et al., 2001). Microglia are the main cellular source of IL-1β in the brain. It is now evident that caspase-1, an essential enzyme for maturation of pro-IL-1β, can be activated through the assembly of a cytosolic protein complex that is known as an inflammasome (Martinon et al., 2002). More recently, the leakage of CB from the lysosomes has been suggested to trigger the activation of the NALP3 inflammasome in microglia/macrophages after phagocytosis of β-amyloid peptides, but not stimulation with ATP (Halle et al., 2008). However, the precise role of leaked CB in the activation of NALP3 inflammasome remains to be determined. Furthermore, there is still evidence suggesting that CB is associated with the maturation of pro-IL-1β in the endosomal/lysosomal system. CB can effectively cleave pro-caspase-1 in a cell-free

Kayo Terada and Jun Yamada contributed equally to this work.

Grant sponsor: Ministry for Education, Science and Culture, Japan; Grant numbers: 17390495, 17659578, 15082204.

*Correspondence to: Hiroshi Nakanishi, Department of Aging Science and Pharmacology, Faculty of Dental Sciences, Kyushu University, Fukuoka 812-8582, Japan. E-mail: nakan@dent.kyushu-u.ac.jp

Received 11 November 2008; Accepted 27 May 2009

DOI 10.1002/glia.20906

Published online 18 June 2009 in Wiley InterScience (www.interscience.wiley.com).

system only at an acidic pH (Vancompernollea et al., 1998) and in THP-1 monocytic cells after stimulation with the microbial toxin nigericin (Hentze et al., 2003). Pretreatment of the animals with CA-074, a specific inhibitor for CB, also inhibits ischemia-induced activation of caspase-1 and caspase-11 in the brain (Benchoua et al., 2004). Furthermore, lysosomotropic agents can also inhibit the release of IL-1β (Weber and Levitz, 2001).

In the present study, the roles of CB in the activation of caspase-1 and the subsequent maturation of IL-1β were examined using microglia prepared from CB-deficient (CB−/−) mice. Chromogranin A (CGA), an acidic glycophosphoprotein localized in the secretory granules of neurons and endocrine cells, was used in the present study as a stimulant for microglia, because CGA can activate pro-caspase-1 in microglia (Kingham and Pocock, 2000) and is implicated in many neurological diseases through activation of microglia and subsequent induction of inflammatory processes (Ciesielski-Treska et al., 1998, 2001; Kingham et al., 1999). CGA is also identified as an endogenous component of neurodegenerative plaques in Alzheimer's disease and Lewy bodies in Parkinson's disease (Wang and Munoz, 1995). The present study provided evidence that CB is involved in the activation of caspase-1 and the subsequent processing of pro-IL-1β in enlarged lysosomes formed after treatment with CGA. Therefore, CB plays a key role in the signaling pathways leading to microglia-induced neuroinflammation in neurological diseases.

MATERIALS AND METHODS

Animals

This study was approved by the Animal Research Committee of the Kyushu University. The heterozygous (+/−) mice with C57/BL background (Halangk et al., 2000) were transferred to the Institute of Experimental Animal Sciences, Kyushu University Faculty of Dentistry, and kept in a specific pathogen-free condition. The selection of CB−/− mice from their littermates, which were obtained by heterozygous coupling, was performed by examining the template genomic DNA that was isolated from tail biopsies, using CB exon 4-specific PCR with the primers of MCB11 (5′-GGTTGCGTTCGG TGAGG-3′) and MCBGT (5′-AACAAGAGCCGCAGGAG C-3′) (Koike et al., 2003).

Microglial Cell Culture

Microglia were isolated from the mixed primary cell cultures from the cerebral cortex of 3-day-old wild-type or CB−/− mice according to the methods described previously (Sastradipura et al., 1998). The purity of microglia was more than 96% as determined by the immunostaining of anti-ionized calcium binding adaptor molecule 1 (Iba1) antibody (Wako Pure Chemical Industries, Osaka, Japan).

Assay for IL-1β and Tumor Necrosis Factor-α (TNF-α)

After treatment with 10 nM CGA, the amounts of IL-1β and TNF-α released from microglia at a density of 5.0×10^5 cells/mL were measured by enzyme-linked immunosorbent assay (ELISA) kits (R&D Systems, Minneapolis, MN) following the protocol provided by manufacturer. The absorbency at 450 nm was performed by using a microplate reader.

Assay for Cell Survival

The culture medium of microglia plated on the 96-well dishes (5×10^5 cells/well) at 48 h after treatment with 10 nM CGA (Peptide Institute, Osaka, Japan) was subjected to the measurement of the cell viability by WST-8 regent that converts to water-soluble formazan by mitochondrial dehydrogenase (Cell counting kit-8, Dojindo, Kumamoto, Japan). Cells were incubated with E-64d (Peptide Institute), CA-074Me (Peptide Institute) pepstatin A (Peptide Institute), benzyloxycarbonyl-DEVD- fluoromethylketone (z-DVD-fmk, Calbiochem, San Diego, CA), benzyoxycarbonyl- YVAD-fluoromethylketon (z-YVAD-fmk, Calbiochem), or N^G-nitro-L-arginine methyl ester (L-NAME, Affinity Bioregents, Golden, CO) 1 h before treatment with CGA. The assay was performed according to the protocol provided by manufacturer. The absorbency at 450 nm was performed by using a microplate reader.

Assay for Total Nitrite

The cells were plated on 96-well dishes at a density of 5×10^4 cells per well. Cells were treated with 10 nM CGA for 48 h. The total nitrite in the supernatant was measured by incubating supernatants with nitrate reductase and βNADPH for 15 min at 37°C before addition of Griess Reagent (Griess Reagent Kit, Dojindo). Griess regent was combined with an equal volume of supernatants and incubated at room temperature for 15 min. The total amount of nitrite was measured spectrophotometrically by using a micro plate reader with the absorbance at 540 nm.

Electrophoresis and Immunoblotting

After treatment with 10 nM CGA in the presence or absence of protease inhibitors that were incubated for 1 h before adding CGA, the cytosolic and cell culture supernatants were collected at various time points. Each sample was electrophoresed using the 15% SDS-polyacrylamide gels. Proteins on SDS gels were transferred electrophoretically to the nitrocellulose membranes. Following blocking, the membranes were incubated at 4°C overnight under gentle agitation with each primary antibody: anti-IL-1β (1:500, Santa Cruz Biotech, Santa

Cruz, CA), anti-CB (1:1,000, Upstate, Lake Placid, NY), anti-caspase-1p 20 (1:500, Santa Cruz Biotech), which recognizes cleavage site of pro-caspase-1, anti-LC-3 (1:1,000, Medical and Biological Lab., Nagoya, Japan), or anti-actin (1:1,000, Santa Cruz Biotech) antibody. After washing, the membranes were incubated with horseradish peroxidase (HRP)-labeled anti-goat (1:1,000, R&D Systems, Mineapolis, MN) or anti-rabbit (1:1,000, Amersham Pharmacia Biotech, Buckinghamshire, UK) antibody for 1 h at room temperature. Subsequently, the membrane-bound, HRP-labeled antibodies were detected by an enhanced chemiluminescence detection system (ECK lit, Amersham Pharmacia Biotech) with an image analyzer (LAS-1000, Fuji Photo Film, Tokyo, Japan).

Real-Time Quantitative RT-PCR

Total RNAs were subjected to the measurement of Rneasy RNA purification kit (Qiagen, Hilden, Germany). To avoid any contamination of genomic DNA, cytoplasmic RNAs were isolated and DNase was added according to the manufacturer's protocol. RT minus controls were run to confirm the presence of genomic contamination. First strand cDNA synthesized from 1 mg of total RNA with random hexamer primers and oligo primers was used as template in each reaction. Syber green based real-time RT-PCR was performed with DyNAmo SYBER Green 2-step qRT-PCR kit (Finnzymes, Espoo, Finland). Rotor Gene 3000 (Corbett Research, Mortlake, Australia) was used for the signal detection. PCR was performed using 1×master mix, 0.5 μM of each primer. For standardization, mouse GAPDH was used. The primers for detection of CB, CD, cathepsin L (CL), GAPDH, cDNAs were as follows: CB (67 bp), 5′- TTGCGTTCGGTGAGGACATAC-3′ and 3′-CGG GCAGTTGGACCATTG-5′; CD (68 bp), 5′-TTCGTCCTC CTTCGCGATT-3′ and 3′-TCCGTCATAGTCCGACGGAT A-5′; CL (70 bp), 5′-TCCTTAAGACCGGCAAACTGAT-3′ and 3′-ATTGCCTTGAGCGTGAGAACA-5′; mouse GAP DH (203 bp), 5′-TGACCACAGTCCATGCCATC-3′ and 3′-GACGGACACATTGGGGGTAG-5′. PCR conditions were 95°C for 15 min, followed by 35 cycles at 94°C for 10 s, 60°C for 20 s, and 72°C for 20 s. After real-time RT-PCR, the reaction products were analyzed by electrophoresis on ethidium bromide, stained agarose gel. All of the PCR experiments were performed in duplicate to verify the results.

Preparation of Frozen Sections

The wild-type and CB−/− mice with the young (3-month-old, $n = 3$ each) and aged (24-month-old, $n = 3$ each) groups were anesthetized with sodium pentobarbital (30 mg/kg, i.p.) and then were perfused intracardially with 0.01 M phosphate-buffered saline (PBS, pH 7.4) and PLP fixative consisting of 0.01 M sodium metaperiodate, 0.075 M L-lysine-HCl, 2% paraformaldehyde (PFA), and 0.03% phosphate buffer (pH 6.2). The brains were removed and immersed in the same fixative for 6 h at 4°C. The specimens were cryoprotected 2 days in 30% sucrose in PBS and then were embedded in an optimal cutting temperature compound (Sakura Finetechnical Co., Tokyo, Japan). Serial coronal frozen sections (10 μm) including the striatum or hippocampus were prepared for immunofluorescent staining.

Immunofluorescent Staining

For primary cultured microglia, the cells were plated on PEI-coated coverslips at the density of 5×10^4 cells per coverslips and were treated with 10 nM CGA for 48 h. Cells were then fixed with 4% PFA. After blocking with 1% bovine serum albumin containing 0.1% Triton-X for 2 h at room temperature, the cells were incubated with each following primary antibodies for 3 days at room temperature: goat anti-IL-1β (1:500, Santa Cruz Biotech), goat anticleaved IL-1β (1:500, Santa Cruz Biotech) that detects the cleavage site of mature IL-1β, rabbit anti-CB (1:2,000), rabbit anti-cathepsin D (CD, 1:2,000), mouse anti-caspase-1 (1:1,000, Calbiochem), rat anti-LAMP-1 (1:1,000, Pharmingen, San Diego, CA) or anti-LC-3 (1:500, MBL, Nagoya, Japan) antibody. After washing with PBS, cells were incubated with following secondary antibodies for 3 h at room temperature: donkey anti-rabbit Alexa488 or donkey anti-goat Alexa 488 or donkey anti mouse Alexa488 and donkey anti-goat Cy3 or donkey anti rat-Cy3 and donkey anti-rabbit Cy5 (1:200, Jackson Immuneresearch, Westgrove, PA) antibody. In some experiments, visualization of the acidic compartment by 3-(2, 4-dinitroanilino)-3′-amino-*N*-methyldipropylamine (DAMP) was carried out using the acidic granule kit (Oxford Biochemical Research, MI) according to the manufacturer's instruction. They were mounted in the antifading medium Vectashield (Vector Lab, Burlingame, CA) and the fluorescence images were observed using a confocal laser scanning microscope (CLSM) (LSM510META, Carl Zeiss, Jena, Germany).

The thin sections were treated with 10% donkey serum for 1 h at room temperature, and then incubated with anticleaved IL-1β antibody (1:100, Santa Cruz Biotech) mixed with rabbit anti-Iba1 antibody overnight at 4°C. After washing with PBS, the sections were incubated with a mixture of FITC- and rhodamine-conjugated secondary antibodies for 1 h at room temperature. The slip was observed using CLSM.

Statistical Analysis

The experimental values are shown as the means ± SE. A paired *t*-test *P*-value of less than 0.05 was considered to indicate statistical significance.

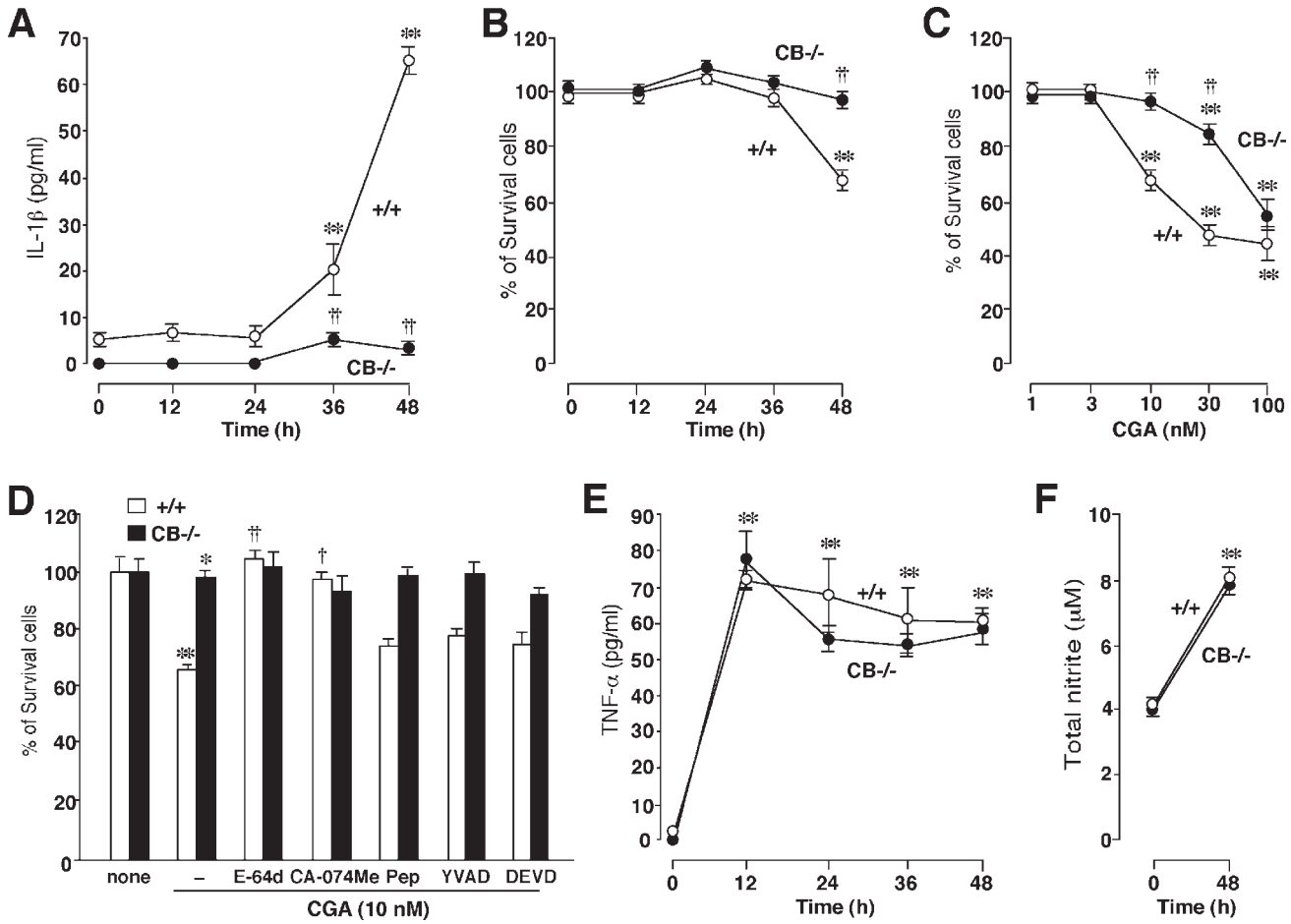

Fig. 1. Inhibitory effects of CB-deficiency on IL-1β secretion from microglia and cell death after treatment with CGA. (**A**) Changes in the mean level of IL-1β in the culture medium of wild-type (+/+) and CB−/− microglia after treatment with 10 nM CGA determined using ELISA assay. Each circle and vertical bar represents the mean and SE of 3–4 experiments. Asterisks and swords indicate a significant difference from microglia left untreated (**$P < 0.01$) and the wild-type cells (††$P < 0.01$), respectively. (**B**, **C**) The time-course (B) and dose–response curve (C) of the mean cell viability of wild-type (+/+) and CB−/− microglia after treatment with 10 nM CGA. Cell viability was determined using WST-8 assay. Each circle and vertical bar represents the mean and SE of 3–4 experiments. Asterisks and swords indicate a significant difference from microglia left untreated (**$P < 0.01$) and the wild-type cells (††$P < 0.01$), respectively. (**D**) Effects of protease inhibitors on CGA-induced decrease in the cell viability of wild-type (+/+) and CB−/− microglia determined using WST-8 assay. E-64d (50 μM), CA-074Me (50 μM), pepstatine A (Pep, 10 μM), z-YVAD-fmk (YVAD, 50 μM), or z-DEVD-fmk (DEVD, 10 μM) was incubated for 24 h before adding CGA. Each column and vertical bar represents the mean and SE of 3–4 experiments. Asterisks and swords indicate a significant difference from microglia left untreated (*$P < 0.05$, **$P < 0.01$) and the CGA-treated cells (†$P < 0.05$, ††$P < 0.01$), respectively. (**E**, **F**) The mean level of TNF-α in the culture medium of wild-type (+/+) and CB−/− microglia after treatment with 10 nM CGA were determined using ELISA assay. Each circle and vertical bar represents the mean and SE of 3–4 experiments. Asterisks indicate a significant difference from microglia left untreated (**$P < 0.01$). (D) The mean total nitrite levels in the supernatants from wild-type (+/+) and CB−/− microglia were determined using Griess regent at 48 h after treatment with 10 nM CGA. Each column and vertical bar represents the mean and SE of 3–4 experiments. Asterisks indicate a significant difference from microglia left untreated (**$P < 0.01$).

RESULTS

The Role of CB in the Release of IL-1β, TNF-α, and Nitric Oxide (NO) by Microglia After Treatment with CGA

The total extracellular level of IL-1β from the primary cultured microglia prepared from CB−/− mice (CB−/− microglia) and wild-type mice (wild-type microglia) after treatment with CGA was examined using an ELISA analysis, which recognizes both the pro and mature forms of IL-1β. The control level of IL-1β in microglia left untreated was very low. After treatment with 10 nM CGA, the initiation of a significant increase in extracellular level of IL-1β was very slow over 36–48 h (Fig. 1A). In contrast, the extracellular level of IL-1β from CB−/− microglia remained at low level even at 48 h after treatment with 10 nM CGA.

At 48 h after treatment with 10 nM CGA, there was a significant decrease in the mean % of survival cell in wild-type but not CB−/− microglia (Fig. 1B). Figure 1C showed a dose–response curve of microglial cell death examined at 48 h after treatment with CGA. 30 nM CGA induced a significant cell death in both wild-type and CB−/− microglia, but the mean % of survival cell in CB−/− microglia was still significantly higher than that in wild-type microglia. In contrast, 100 nM CGA induced ~50% of cell death in both wild-type and CB−/− mice

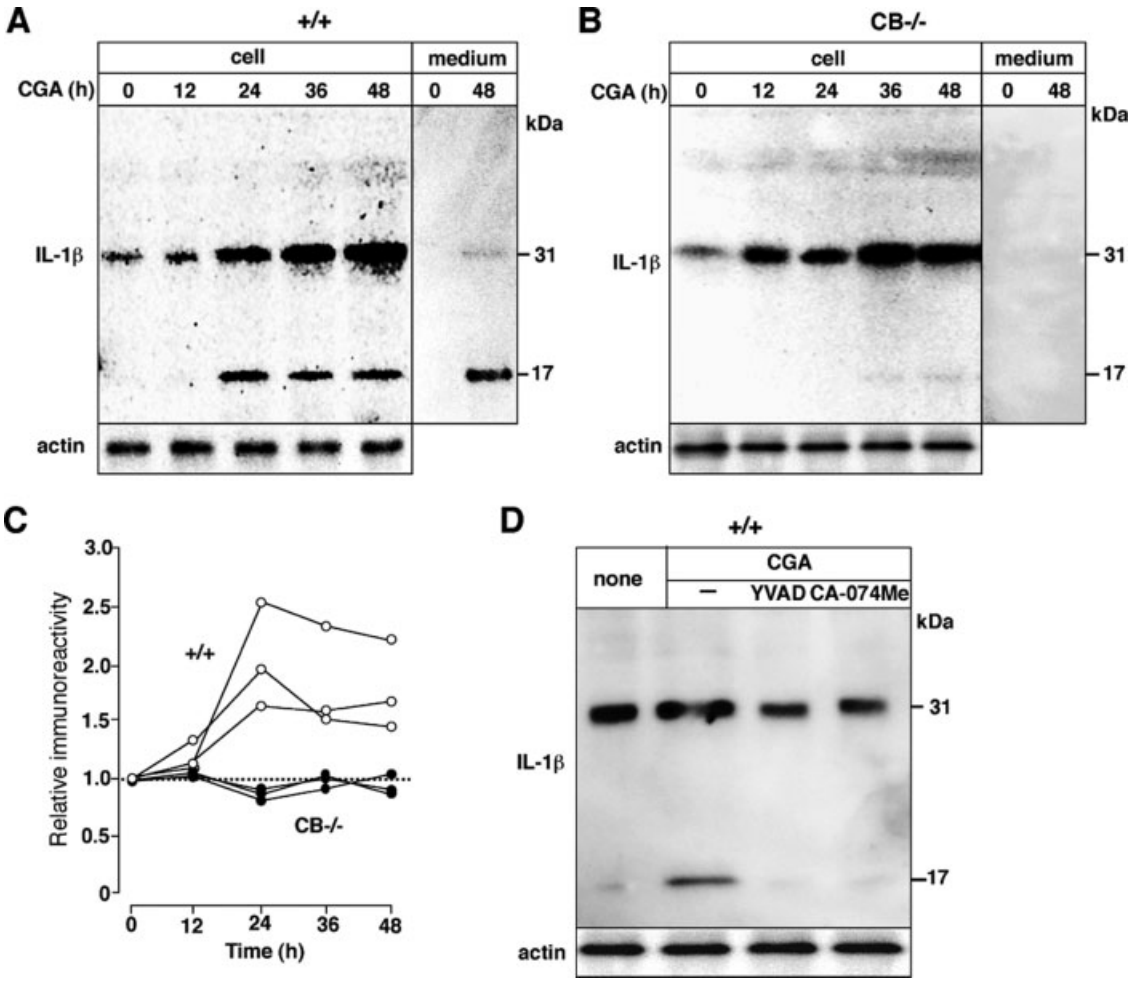

Fig. 2. Inhibitory effects of CB-deficiency on the processing and secretion of IL-1β from microglia after treatment with CGA. (**A**, **B**) Immunoblot analyses for IL-1β in cell lysates and culture medium of wild-type (+/+) microglia (A) and CB−/− microglia (B) after treatment with 10 nM CGA. (**C**) Changes in the relative amounts of mature IL-1β secreted from wild-type microglia (+/+, open circles) and CB−/− microglia (filled circles) after treatment with 10 nM CGA. (**D**) Effects of z-YVAD-fmk (YVAD, 50 μM) or CA-074Me (50 μM) on the CGA-induced maturation of IL-1β in wild-type (+/+) microglia. Inhibitors were applied for 24 h before adding CGA. At 36 h after treatment with 10 nM CGA, the cell lysates were subjected to the immunoblot analysis.

and there was no significant difference in the mean % of survival cell between these two groups. E-64d (50 μM), a broad cysteine protease inhibitor and CA-074Me (50 μM), a specific inhibitor for CB, significantly inhibited the cell death of wild-type microglia induced by 10 nM CGA (Fig. 1D). In contrast, either pepstatine A (10 μM), a specific inhibitor for aspartic proteases, z-YVAD-fmk (50 μM), a specific inhibitor for caspase-1, z-DEVD-fmk (10 μM), a specific inhibitor for caspase-3 (Fig. 1D), or L-NAME (100 μM), NO synthase inhibitor, had no effect on 10 nM CGA-induced microglial cell death (data not shown).

The effects of CB-deficiency on the levels of TNF-α and NO secreted from microglia induced by 10 nM CGA were further examined. As shown in Fig. 1E,F, there was no significant difference in either the mean level of TNF-α or total nitrite in the culture medium of wild-type and CB−/− microglia after treatment with 10 nM CGA.

Involvement of CB in the Proteolytic Processing of Pro-IL-1β into Mature IL-1β in Microglia After Treatment with CGA

Next, the involvement of CB in the proteolytic processing and release of IL-1β by microglia was further examined by immunoblot analyses. IL-1β was produced as the proform with an apparent molecular mass of 31 kDa and pro-IL-1β increased after treatment with 10 nM CGA in both wild-type and CB−/− microglia (Fig. 2A,B). At 24 h after treatment with 10 nM CGA, the 17 kDa mature form of IL-1β became visible in the cell lysates of wild-type microglia (Fig. 2A,C). The amount of the mature IL-1β in the cell lysates peaked at 24 h after treatment with 10 nM CGA. In the culture medium, the mature IL-1β was detected at 48 h after treatment with 10 nM CGA. In contrast, the mature form was not observed in either the cell lysates or the culture medium of CB−/− microglia even at 48 h after

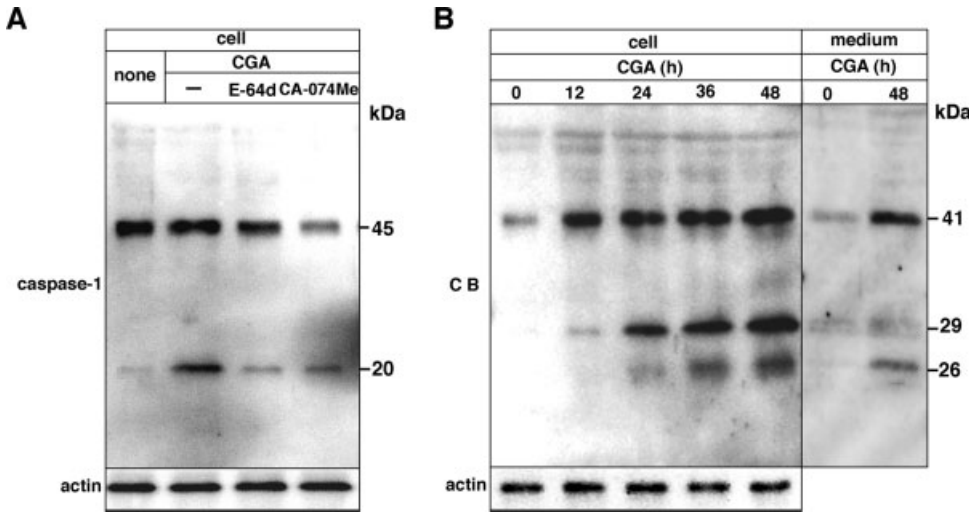

Fig. 3. Processing of caspase-1 and CB in wild-type microglia after treatment with CGA. (**A**) Effects of E-64d (50 μM) and CA-074Me (50 μM) on CGA-induced maturation of caspase-1. At 36 h after treatment with 10 nM CGA, the cell lysates were subjected to the immunoblot analysis. (**B**) Immunoblot analyses of CB in the cell lysates and culture medium of wild-type microglia after treatment with 10 nM CGA.

treatment with 10 nM CGA (Fig. 2B,C). Furthermore, the proteolytic processing of pro-IL-1β to its mature form was completely inhibited by z-YVAD-fmk (50 μM) or CA-074Me (50 μM) in wild-type microglia (Fig. 2D). These results strongly suggest that the maturation of pro-IL-1β in CGA-stimulated microglia is dependent on the enzymatic activities of both CB and caspase-1.

Increased Expression of CB and Activation of Caspase-1 in Microglia After Treatment with CGA

To further address a possible involvement of CB in the activation of pro-caspase-1, the effects of inhibitors for CB were examined on the processing of pro-caspase-1. Figure 3A shows that pro-caspase-1 (45 kDa) was proteolytically processed into the mature enzyme (20 kDa) after treatment with 10 nM CGA in wild-type microglia as reported by Kingham and Pocock (2000). This conversion was markedly inhibited by E-64d (50 μM) or CA-074Me (50 μM). These observations strongly suggest the involvement of CB in the activation of pro-caspase-1.

Next, the changes in the amount and localization of CB in microglia after treatment with CGA were analyzed. CB was observed mainly as a polypeptide with an apparent molecular mass of 41 kDa, which corresponded well with that of pro-CB. CGA induced synthesis and processing of pro-CB in wild-type microglia over 12–48 h. At 12 h after treatment with 10 nM CGA, the processed single-chain form of CB with 29 kDa became visible (Fig. 3B). At 24 h after the treatment, the protein band with an apparent mass of 26 kDa also became visible. The 26 kDa-protein corresponds to the heavy chain of the two-chain enzyme yielded by further processing of the single-chain enzyme. The proteolytic processing of the single-chain enzyme as well as pro-CB takes place in the lysosomes (Nishimura and Kato, 1987). The time course of pro-CB maturation corresponded closely with that of pro-IL-1β maturation (Fig. 3B), therefore further suggesting the involvement of CB in the processing of pro-IL-1β. In the culture medium, pro-CB as well as its mature form was detected at 48 h after treatment with CGA.

Changes in mRNA Levels of CB, CD, and CL in Microglia After Treatment with CGA

Next, real-time quantitative RT-PCR was performed to examine changes of mRNA levels of CB and other cathepsins, CD and CL, after treatment with 10 nM CGA. mRNA of CB, CD, and CL were detected in wild-type microglia (Fig. 4A). At 24–36 h after treatment with 10 nM CGA, the mean level of CB mRNA significantly increased to ~177.7% ± 14.4% in comparison to that of untreated wild-type microglia (Fig. 4B). There was no significant change in the mean level of either CD or CL mRNA after treatment with 10 nM CGA. In contrast, the expression of both CD and CL in CB−/− microglia significantly increased after treatment with CGA. The mean levels of CD and CL mRNA in CGA-treated CB−/− microglia increased to 356.7% ± 84.1% and 593.8% ± 128.7%, respectively, in comparison to that of untreated CB−/− microglia (Fig. 4B).

Subcellular Localization of CB and Caspase-1 in LAMP-1-Positive Acidic Compartments of Microglia After Treatment with CGA

Triple immunofluorescent staining that combined visualization of CB, LAMP-1, and caspase-1 was conducted to assess a possible co-localization of CB and caspase-1 in lysosomes of CGA-stimulated wild-type microglia.

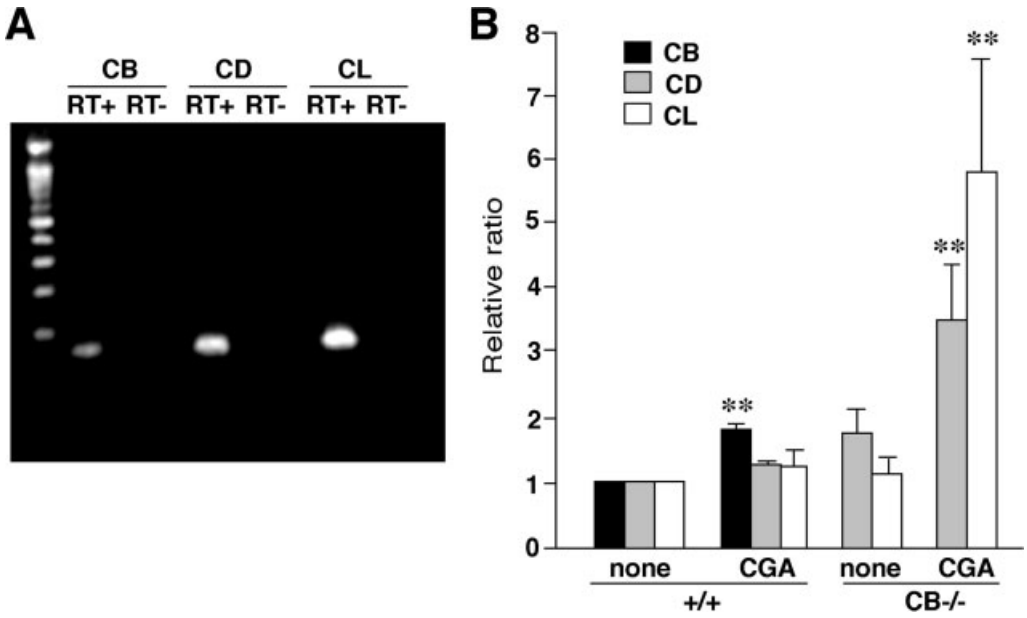

Fig. 4. Changes in the expression levels of CB, CD, and CL in the primary cultured microglia after treatment with CGA. (**A**) RT-PCR was performed on mRNA from wild-type microglia to examine the expression of CB, CD, and CL mRNA. CB (67 bp), CD (68 bp), and CL (70 bp) were detected. 1 lane; CB RT(+), 2 lane; CB RT(−), 3 lane; CD RT(+), 4 lane; CD RT(−), 5 lane; CL RT(+), 6 lane CL RT(−). RT(−) is reverse transcriptase free. This lane confirmed the no DNA commingling. (**B**) The normalized expression levels of CB, CD, and CL in wild-type (+/+) and CB−/− microglia at 48 h after treatment with 10 nM CGA by quantitative real-time RT-PCR. Each column and vertical bar represents the mean and SE of 3–4 experiments, respectively. Asterisks indicate a significant difference from microglia left untreated (**$P < 0.01$).

Untreated wild-type microglia showed relatively small granular immunoreactivity for CB that corresponded with that for LAMP-1 (Fig. 5A). However, there was only a faint immunoreactivity for caspase-1. After treatment with 10 nM CGA, CB-containing enlarged vesicles were formed (Fig. 5B). The mean size was 4.2 μm (range: 3.5–6.3 μm). These enlarged vesicles were encircled by a LAMP-1-positive membrane, thus suggesting their endosomal/lysosomal origins. The immunoreactivity for LC3 did not correspond with that for LAMP-1 in wild-type microglia, suggesting that autophagy was not involved in the formation of the enlarged lysosomes (data not shown). In addition, a large granular immunoreactivity for caspase-1 was also observed in CGA-treated microglia. The immunoreactivity for caspase-1 closely corresponded with that for CB in these enlarged LAMP-1-positive lysosomes.

To examine the acidic nature of the enlarged LAMP-1-positive lysosomes that contained both CB and caspase-1, wild-type microglia treated with 10 nM CGA were subsequently incubated with DAMP, which is a basic congener of dinitrophenol and accumulates in acidic organelles (Anderson et al., 1984). After 3 h of incubation with DAMP, the cells were fixed and stained for DAMP using anti-dinitrophenol antibody. DAMP staining was also combined with staining for both CB and caspase-1. The immunoreactivity for CB corresponded closely with that for DMAP, but the immunoreactivity for caspase-1 was very faint in untreated wild-type microglia (Fig. 5C). In contrast, large granular immunoreactivity for CB corresponded closely with that for both DMAP and caspase-1 in CGA-treated wild-type microglia (Fig. 5D).

Subcellular Localization of the Cleaved IL-1β in Microglia After Treatment with CGA

The localizations of the mature IL-1β in untreated and CGA-treated microglia were next examined using anticleaved IL-1β antibody that detects the cleavage site of mature IL-1β. There was only a faint immunoreactivity for the cleaved IL-1β in the cytoplasm of the untreated wild-type microglia (Fig. 6A). At 36 h after treatment with 10 nM CGA, large granular immunoreactivity for the cleaved IL-1β appeared in the cytoplasm of microglia (Fig. 6B). The large granular immunoreactivity for the cleaved IL-1β corresponded with LAMP-1-positive enlarged lysosomes. In CB−/− microglia, CGA also induced enlarged LAMP-1-positive lysosomes that contained CD (Fig. 6C). However, the immunoreactivity for the cleaved IL-1β was barely detectable in these CD-positive enlarged lysosomes of CGA-treated CB−/− microglia (Fig. 6D).

Triple immunofluorescent staining that combined visualization of CB, caspase-1, and the cleaved IL-1β was conducted to assess the possible co-localization of CB, caspase-1, and the cleaved IL-1β in enlarged lysosomes of CGA-treated wild-type microglia. In wild-type microglia left untreated, immunoreactivity for either caspase-1

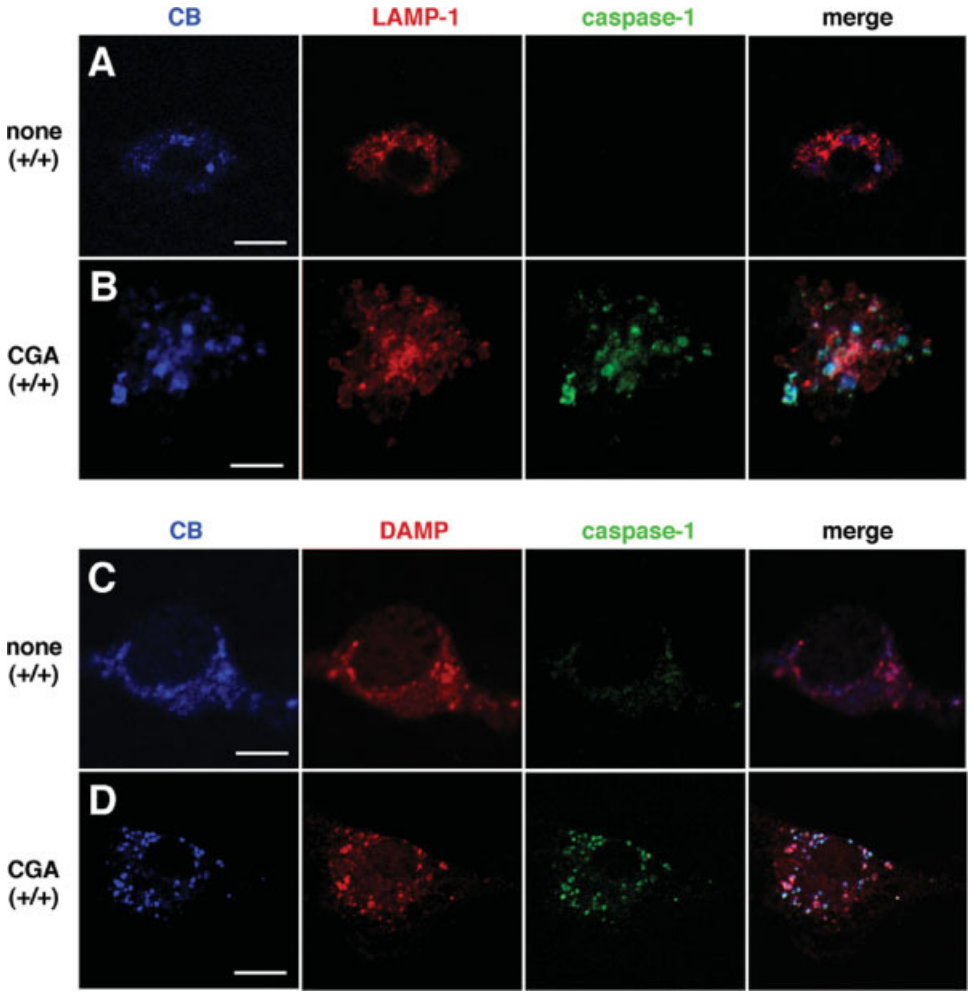

Fig. 5. Increased expression and co-localization of CB and caspase-1 in enlarged acidic LAMP-1-positive lysosomes of wild-type microglia at 36 h after treatment with 10 nM CGA. (**A**, **B**) Immunofluorescent CLSM images for CB, LAMP-1, and caspase-1 in untreated (A) and CGA-treated (B) wild-type microglia. Scale bars = 5 μm. (**C**, **D**) Immunofluorescent CLSM images for CB, DAMP, and caspase-1 in untreated (C) and CGA-treated (D) wild-type microglia. Scale bars = 5 μm.

or the cleaved IL-1β was barely detectable (Fig. 6E). In contrast, large granular immunoreactivity for CB, caspase-1 and the cleaved IL-1β both closely corresponded (Fig. 6F).

Effects of CB-deficiency on IL-1β Expression in the Hippocampus of Aged Mice

Finally, the effects of CB-deficiency on the expression of IL-1β in microglia were further investigated in *in vivo*. The effects of CB-deficiency on the expression of IL-1β in the hippocampus were investigated in the aged mice, because the expression level of IL-1β significantly increases during aging (Griffin et al., 2006; Hayashi et al., 2008). In consistent with previous observations, microglia were found to express intense granular immunoreactivity for the cleaved IL-1β in the hippocampus of the aged mice (Fig. 7A). In contrast, there was no observable expression of the cleaved IL-1β in the hippocampus of the aged CB−/− mice (Fig. 7B).

DISCUSSION

Considering that proteases can irreversibly cleavage peptide bonds, functions of proteases can be classified into two major categories. One is their "disintegrating action" by which physiological functions of substrate are inactivated. The other is their "modulatory action" by which substrate are activated after cleavage. In the present study, CB-deficiency was found to abrogate CGA-induced maturation of pro-IL-1β and its release from microglia. Furthermore, the activation of caspase-1 was inhibited by CA-074Me, a specific inhibitor for CB. Therefore, the present study provides the evidence that CB plays a key role in the maturation of pro-IL-1β through the activation of caspase-1 in CGA-stimulated microglia.

CGA was also found to induce gene expression and increased synthesis of CB in microglia. CB was synthesized as a proform and it was processed to two-chain forms, light and heavy chains through a single-chain form. Both the single and heavy chains of the two-chain

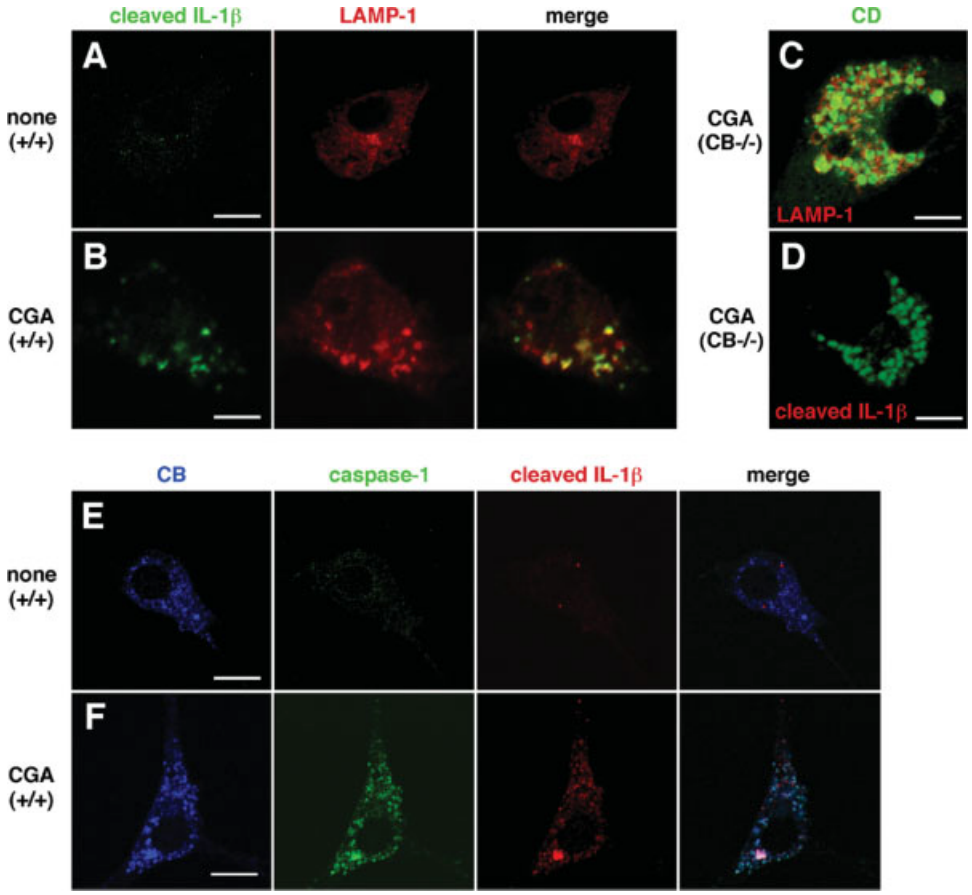

Fig. 6. Increased expression of the cleaved IL-1β and co-localization with CB and caspase-1 in enlarged lysosomes of microglia at 36 h after treatment with 10 nM CGA. (**A**, **B**) Immunofluorescent CLSM images for the cleaved IL-1β and LAMP-1 in untreated (A) and CGA-treated (B) wild-type microglia. Scale bars = 5 μm. (**C**, **D**) Immunofluorescent CLSM images for CD and merge with those for LAMP-1 (C) and the cleaved IL-1β (D) in CGA-treated CB−/− microglia. Scale bars = 5 μm. (**E**, **F**) Immunofluorescent CLSM images for CB, cspase-1, and the cleaved IL-1β in untreated (E) and CGA-treated (F) wild-type microglia. Scale bars = 5 μm.

enzymes were first visible at 24 h after treatment with CGA. Considering that the proteolytic processing of the single-chain enzyme as well as pro-CB takes place in the lysosomes (Nishimura and Kato, 1987), pro-CB was fully sorted into lysosomes of microglia at 24 h after treatment with CGA. The maturation of pro-CB correlated with the appearance of mature IL-1β in the cytoplasm of CGA-stimulated microglia. CGA also significantly increased the mean mRNA level of CB but not CD or CL in wild-type microglia. It is conceivable, therefore, the gene expression and increased synthesis of CB are the rate limiting steps for the activation of caspase-1 and subsequent maturation of IL-1β in microglia. It is of particular interest that the mean mRNA levels of both CD and CL markedly increased in CB−/− microglia after treatment with CGA. This may represent a cellular compensatory response to a primary CB-deficiency that causes a lysosomal dysfunction.

In the present study, extracellular IL-1β could be detected without any significant cell death at 36 h after treatment with 10 nM CGA, suggesting that extracellular IL-1β was mainly caused by secretion rather than leakage because of cell lysis. CGA-induced microglial

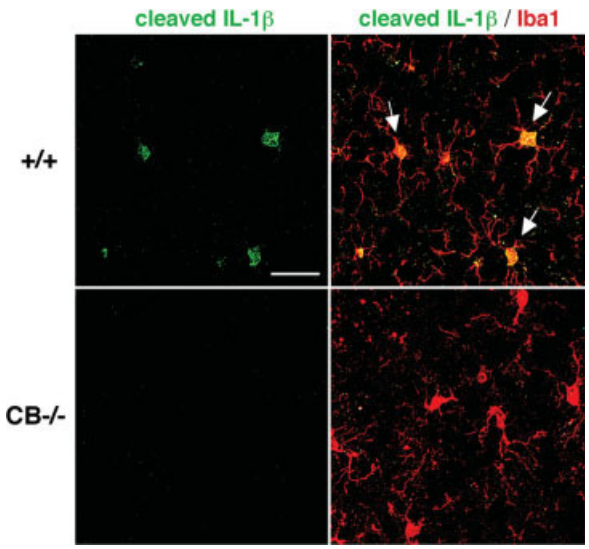

Fig. 7. Inhibitory effects of CB-deficiency on IL-1β expression in the hippocampus of the aged mice. Immunofluorescent CLSM images for cleaved IL-1β and merge with those for Iba1 in the hippocampus of the aged wild-type (+/+, **A**) and CB−/− mice (**B**). Scale bar = 20 μm.

cell death is significantly depressed due to both the CB-deficiency and the presence of CA074Me, a specific inhibitor for CB. In contrast, z-YVAD-fmk, a specific inhibitor for caspase-1 failed to inhibit CGA-induced microglial cell death. Our observations further suggest the existence of two differential death pathways, which depend on the concentration of CGA. At a relatively low concentration (e.g., 10 nM), CGA induced CB-dependent and NO-independent nonapoptotic death pathway. At a relatively high concentration (e.g., 100 nM), CGA induced CB-independent cell death pathway. In contrast, Kingham et al. (1999) reported that the caspase-1-mediaed apoptotic pathway was responsible for 10 nM CGA-induced microglial cell death. Furthermore, they also demonstrated that CGA-induced microglial cell death was dependent on the NO production. One possible explanation for this discrepancy is the difference in the species used for the preparation of the primary cultured microglia (rat vs. mouse). The sensitivity of primary cultured rat microglia used by Kingham et al. (1999) to CGA may be ~10 times higher than that of the murine microglia under our culture conditions.

The typical size of the primary lysosomes is below 1 μm in diameter, whereas the mean diameter of CB-containing enlarged lysosomes in CGA-stimulated microglia was 4.2 μm. Furthermore, DAMP staining clearly showed that CB-positive enlarged lysosomes were acidic compartments. Therefore, it is considered that both procaspase-1 and pro-IL-1β in the cytoplasm are trapped by these CB-containing acidic enlarged lysosomes during the process of their formation, and then pro-IL-1β is processed to the mature form. These present findings are consistent with previous observations that IL-1β and CD colocalized within endolysosome-related vesicles, and that the secretion of IL-1β involves exocytosis of these vesicles in LPS-activated human monocytes (Andrei et al., 1999). Andrei et al. (2004) further reported that the secretory lysosomes are the site of ATP-induced IL-1β processing in LPS-activated monocytes. More recently, Qu et al. (2007) demonstrated that pro-IL-1β was processed to the mature form in the endosome-derived recycling multivesicular bodies in murine bone marrow-derived macrophages. These multivesicular bodies, which entrapped IL-1β and caspase-1, are released as exosomes. In contrast, Brough and Rothwell (2007) demonstrated that pro-IL-1β was processed to the mature form in the cytosol of murine macrophages after stimulation with LPS, and further proposed that IL-1β directly passes through the plasma membrane via molecularly undefined protein transporters. There were also reports contradictory to these observations showing that mature IL-1β was not expressed in cell lysates of rat microglia (Chauvet et al., 2001), murine macrophage (Beuscher et al., 1990), and human monocytes (Singer et al., 1995) after stimulation with LPS. The reasons for these discrepancies are unclear, but the different experimental conditions including cell types, species and concentrations of stimulants used for cellular activation, can be possible explanations. Taken together, the maturation and secretion of IL-1β are complicated events that are influenced by these factors.

Recently, much attention has been paid on the modulatory action of leaked CB in the cytoplasm. Nigericin induces lysosomal leakage, translocation and activation of CB, which simultaneously induces both caspase-1 activation and cell death in THP-1 monocytes (Hentze et al., 2003). More recently, Halle et al. (2008) demonstrated that microglial phagocytosis of Aβ induces lysosomal enlargement and loss of lysosomal integrity, which leads to release of CB into the cytoplasm. They showed that the overall cellular staining pattern of CB seemed diffuse and less punctate and was outside LAMP-1-positive enlarged lysosomes. The release of CB is causally related with the NALP3 inflammasome activation. In contrast, our observations clearly indicate that CB localized in LAMP-1-positive enlarged lysosomes of CGA-stimulated microglia and there was no sign for the leakage of CB. Furthermore, immunoreactivity for the cleaved IL-1β localized in the enlarged lysosomes, which contained both CB and caspase-1. It is noteworthy that the enlarged lysosomes localized in the margins of the cells were devoid of CB and they appeared to fuse with the plasma membrane. Moreover, the mature form of CB was detected in the culture medium after treatment with CGA. Therefore, it is thus thought that activation of caspase-1 and the subsequent IL-1β maturation occurred exclusively in enlarged lysosomes of CGA-stimulated microglia and their contents are released by exocytosis.

In line with our observations using primary cultured microglia, intense immunoreactivity for the cleaved IL-1β was detected in the hippocampus of the aged wild-type but not CB−/− mice. There is increasing evidence that neuroinflammation mediated by activated microglia plays a major causative role in age-dependent deficit of the working memory and the hippocampal long-term potentiation (Gemma et al., 2005; Griffin et al., 2006; Hayashi et al., 2008). In our preliminary experiments, the mean magnitude of long-term potentiation in the Schaffer collateral-CA1 synapses of CB−/− mice was significantly larger than that of wild-type mice. Therefore, further studies are needed to examine the possible reversal effect of CB-deficiency on the age-dependent deficits of memory.

REFERENCES

Allan SM, Tyrrell PJ, Rothwell NJ. 2005. Interleukin-1 and neuronal injury. Nat Rev Immunol 5:629–640.

Anderson RGW, Falck JR, Goldstein JL, Brown MS. 1984. Visualization of acidic organelles in intact cells by electron microscopy. Proc Natl Acad Sci USA 81:1107–1122.

Andrei C, Dazzi C, Lotti L, Torrisi MR, Chumini G, Rubartelli A. 1999. The secretory route of the leaderless protein interleukin 1β involves exocytosis of endolysosome-related vesicles. Mol Biol Cell 10:1463–1475.

Andrei C, Margiocco P, Poggi A, Lotti LV, Torrisi MR, Rubartelli A. 2004. Phospholipases C, A_2 control lysosome-mediated IL-1β secretion: Implications for inflammatory processes. Proc Natl Acad Sci USA 101:9745–9750.

Benchoua A, Braudeau J, Reis A, Couriaud C, Onténiente B. 2004. Activation of proinflammatory caspases by cathepsin B in focal cerebral ischemia. J Cereb Blood Flow Metab 24:1272–1279.
Beuscher HU, Gunther C, Rollinghoff M. 1990. IL-1β is secreted by activated murine macrophages as biologically inactive precursor. J Immunol 144:2179–2183.
Brough D, Rothwell NJ. 2007. Caspase-1-dependent processing of pro-interleukin-1β is cytosolic and precedes cell death. J Cell Sci 120:772–781.
Cardozo C, Padilla ML, Choi HS, Lesser M. 1992. Goblet cell hyperplasia in large intrapulmonary airways after intratracheal injection of cathepsin B into hamsters. Am Rev Respir Dis 145:675–679.
Chauvet N, Palin K, Verrier D, Poole S, Dantzer R, Lestage J. 2001. Rat microglial cells secrete predominantly the precursor of interleulin-1β in response to lipopolysaccharide. Eur J Neurosci 14:609–617.
Ciesielski-Treska J, Ulrich G, Chasserot-Golaz S, Zwiller J, Revel MO, Aunis D, Bader MF. 2001. Mechanisms underlying neuronal death induced by chromogranin A-activated microglia. J Biol Chem 276:13113–13120.
Ciesielski-Treska J, Ulrich G, Taupenot L, Chasserot-Golaz S, Corti A, Aunis D, Bader MF. 1998. Chromogranin A induces a neurotoxic phenotype in brain microglial cells. J Biol Chem 273:14339–14346.
Gan L, Ye S, Chu A, Anton K, Yi S, Vincent VA, von Schack D, Chin D, Murray J, Lohr S, Patthy L, Gonzalez-Zulueta M, Nikolich K, Urfer R. 2004. Identification of cathepsin B as a mediator of neuronal death induced by Aβ-activated microglial cells using a functional genomics approach. J Biol Chem 279:5565–5572.
Gemma C, Fister M, Hudson C, Bickford PC. 2005. Improvement of memory for context by inhibition of caspase-1 in aged rats. Eur J Neurosci 22:1751–1756.
Griffin R, Nally R, Nolan Y, McCartney Y, Linden J, Lynch MA. 2006. The age-related attenuation in long-term potentiation is associated with microglial activation. J Neurochem 99:1263–1272.
Guo W, Wang H, Watanabe M, Shimizu K, Zou S, LaGraize SC, Wei F, Dubner R, Ren K. 2007. Glial-cytokine-neuronal interactions underlying the mechanisms of persistent pain. J Neurosci 27:6006–6018.
Halangk W, Lerch MM, Brandt-Nedelev B, Roth W, Ruthenbuerger M, Reinheckel T, Domschke W, Lippert H, Peters C, Deussing J. 2000. Role of cathepsin B in intracellular trypsinogen activation and the onset of acute pancreatitis. J Clin Invest 106:773–781.
Halle A, Hornung V, Petzold GC, Stewart CR, Monks BG, Reinheckel T, Fitzgerald KA, Latz E, Moore KJ, Golenbock DT. 2008. The NALP3 inflammasome is involved in the innate immune response to amyloid-β. Nat Immunol 9:857–865.
Hashimoto Y, Kakegawa H, Narita Y, Hachiya Y, Hayakawa T, Kos J, Turk V, Katunuma N. 2001. Significance of cathepsin B accumulation in synovial fluid of rheumatoid arthritis. Biochem Biophys Res Commun 282:334–339.
Hayashi Y, Yoshida M, Yamato M, Ide T, Wu Z, Ochi-Shindou M, Kanki T, Kang D, Sunagawa K, Tsutsui H, Nakanishi H. 2008. Reverse of age-dependent memory impairment and mitochondrial DNA damage in microglia by an overexpression of human mitochondrial transcription factor A in mice. J Neurosci 28:8624–8634.
Hentze H, Lin XY, Choi MSK, Porter AG. 2003. Critical role for cathepsin B in mediating caspase-1-dependent interleukin-18 maturation and caspase-1-independent necrosis triggered by the microbial toxin nigericin. Cell Death Diff 10:956–968.
Kawasaki Y, Xu ZZ, Wang X, Park JY, Zhuang ZY, Tan PH, Gao YJ, Roy K, Corfas G, Lo EH, Ji RR. 2008. Distinct roles of matrix metalloproteases in the early- and late-phase development of neuropathic pain. Nat Med 14:331–336.
Kingham PJ, Cuzner ML, Pocock JM. 1999. Apoptotic pathways mobilized in microglia and neurons as a consequence of chromogranin A-induced microglial activation. J Neurochem 73:538–547.
Kingham PJ, Pocock JM. 2000. Microglial apoptosis induced by chromogranin A is mediated by mitochondrial depolarization and permeability transition but not by cytochrome *c* release. J Neurochem 74:1452–1462.
Kingham PJ, Pocock JM. 2001. Microglial secreted cathepsin B induces neuronal apoptosis. J Neurochem 76:1475–1484.
Koike M, Shibata M, Ohsawa Y, Nakanishi H, Koga T, Kametaka S, Waguri S, Momoi T, Kominami E, Saftig P, Peters C, Kurt von Figura, Uchiyama Y. 2003. Involvement of two different cell death pathways in retinal atrophy of cathepsin D-deficient mice. Mol Cell Neurosci 22:146–161.
Martinon F, Burns K, Tschopp J. 2002. The inflammasome: A molecular platform triggering activation of inflammatory caspases and processing of proIL-1β. Mol Cell 10:417–426.
Mueller-Steiner S, Zhou Y, Arai H, Roberson ED, Sun B, Chen J, Wang X, Yu G, Esposito L, Mucke L, Gan L. 2006. Antiamyloidogenic and neuroprotective functions of cathepsin B: Implications for Alzheimer's disease. Neuron 51:703–714.
Nakanishi H. 2003. Microglia functions and proteases. Mol Neurobiol 27:163–176.
Nishimura Y, Kato K. 1987. Intracellular transport and processing of lysosomal cathepsin B. Biochem Biophys Res Commun 148:254–259.
Nishioku T, Hashimoto K, Yamashita K, Liou SY, Kagamiishi Y, Maegawa H, Katsube N, Peters C, von Figura K, Saftig P, Katunuma N, Yamamoto K, Nakanishi H. 2002. Involvement of cathepsin E in exogenous antigen processing in primary cultured murine microglia. J Biol Chem 277:4816–4822.
Qu Y, Franchi L, Nunez G, Dubyak GR. 2007. Nonclassical IL-1 β secretion stimulated by P2X7 receptors is dependent on inflammasome activation and correlated with exosome release in murine macrophages. J Immunol 179:1913–1925.
Samad TA, Moore KA, Sapirstein A, Billet S, Allchorne A, Poole S, Bonventre JV, Woolf CJ. 2001. Interleukin-1β-mediated induction of cox-2 in the CNS contributes to inflammatory pain hypersensitivity. Nature 410:471–475.
Sastradipura DF, Nakanishi H, Tsukuba T, Nishishita K, Sakai H, Kato Y, Gotow T, Uchiyama Y, Yamamoto K. 1998. Identification of cellular compartments involved in processing of cathepsin E in primary cultures of rat microglia. J Neurochem 70:2045–2056.
Singer II, Scott S, Chin J, Bayne EK, Limjuco G, Weidner J, Miller DK, Chapman K, Kostura MJ. 1995. The interleukin-1β-converting enzyme (ICE) is localized on the external cell surface membranes and in the cytoplasm ground substance of human monocytes by immuno-electron microscopy. J Exp Med 182:1447–1459.
Vancompernolle K, Van Herreweghe F, Pynaert G, Van de Craen M, De Vos K, Totty N, Sterling A, Fiers W, Vandenabeele P, Grooten J. 1998. Atractyloside-induced release of cathepsin B, a protease with caspase-processing activity. FEBS Lett 438:150–158.
Wang D, Munoz DG. 1995. Qualitative and quantitative differences in senile plaque dystrophic neuritis of Alzheimer's disease and normal aged brain. J Neuropathol Exp Neurol 54:548–556.
Weber SM, Levitz SM. 2001. Chloroquine antagonizes the proinflammatory cytokine response to opportunistic fungi by alkalizing the fungal phagolysosome. J Infect Dis 183:935–942.